Note: This is a draft of a paper submitted for publication. Contents of this paper should not be quoted or referred to without permission of the author(s).

Field Emission from Carbon Films Deposited by Controlled-Low-Energy Beams and CVD Sources

D. H. Lowndes,[1] V. I. Merkulov,[1] L. R. Baylor,[2] G. E. Jellison, Jr.,[1] D. B. Poker,[1] S. Kim,[3] M. H. Sohn,[3] and N. W. Paik[4]

[1]Solid State Division, Oak Ridge National Laboratory, Oak Ridge, TN
[2]Fusion Energy Division, Oak Ridge National Laboratory, Oak Ridge, TN
[3]SKION Corporation, 50 Harrison St., Hoboken, NJ 07030
[4]Physics and Engineering Physics Dept., Stevens Inst. of Technology, Hoboken, NJ 07030

FIELD EMISSION FROM CARBON FILMS DEPOSITED BY CONTROLLED-LOW-ENERGY BEAMS AND CVD SOURCES

DOUGLAS H. LOWNDES*, VLADIMIR I. MERKULOV*, L. R. BAYLOR**, G. E. JELLISON, JR.*, D. B. POKER*, S. KIM†, M. H. SOHN†, and N. W. PAIK††

* Solid State Division, Oak Ridge National Laboratory, Oak Ridge, TN 37831-6056

** Fusion Energy Division, Oak Ridge National Laboratory, Oak Ridge, TN 37831-8071

† SKION Corporation, 50 Harrison St., Hoboken, NJ 07030

†† Physics and Engineering Physics Dept., Stevens Institute of Technology, Hoboken, NJ 07030

ABSTRACT

The principal interests in this work are energetic-beam control of carbon-film properties and the roles of doping and surface morphology in field emission. Carbon films with variable sp^3-bonding fraction were deposited on n-type Si substrates by ArF (193 nm) pulsed-laser ablation (PLA) of a pyrolytic graphite target, and by direct metal ion beam deposition (DMIBD) using a primary Cs^+ beam to generate the secondary C^- deposition beam. The PLA films are undoped while the DMIBD films are doped with Cs. The kinetic energy (KE) of the incident C atoms/ions was controlled and varied over the range from ~25 eV to ~175 eV. Earlier studies have shown that C films' sp^3-bonding fraction and diamond-like properties can be maximized by using KE values near 90 eV. The films' surface morphology, sp^3-bonding fraction, and Cs-content were determined as a function of KE using atomic force microscopy, TEM/EELS, Rutherford backscattering and nuclear reaction measurements, respectively. Field emission (FE) from these very smooth undoped and Cs-containing films is compared with the FE from two types of deliberately nanostructured carbon films, namely hot-filament chemical vapor deposition (HF-CVD) carbon and carbon nanotubes grown by plasma-enhanced CVD. Electron field emission (FE) characteristics were measured using ~25-µm, ~5-µm and ~1-µm diameter probes that were scanned with ~75 nm resolution in the x-, y-, and z-directions in a vacuum chamber (~5 x 10^{-7} torr base pressure) equipped with a video camera for viewing. The hydrogen-free and very smooth a-D or a-C films (with high or low sp^3 content, and with or without ~1% Cs doping) produced by PLD and DMIBD are not good field emitters. Conditioning accompanied by arcing was required to obtain emission, so that their subsequent FE is characteristic of the arc-produced damage site. However, deliberate surface texturing can eliminate the need for conditioning, apparently by geometrical enhancement of the local electric field. But the most promising approach for producing macroscopically flat FE cathodes is to use materials that are highly nanostructured, either by the deposition process (e.g. HF-CVD carbon) or intrinsically (e.g. carbon nanotubes). HF-CVD films were found to combine a number of desirable properties for FE displays and vacuum microelectronics, including the absence of conditioning, low turn-on fields, high emission site density, and apparent stability and durability during limited long-term testing. Preliminary FE measurements revealed that vertically aligned carbon nanotubes are equally promising.

INTRODUCTION

There is currently worldwide interest in developing electron-emitting cathode materials for (cold) field emission (FE) displays [1] and other vacuum microelectronics devices [2]. The four principal requirements for a practical FE material are a low emission turn-on (or threshold) electric field, E_{th}, a sufficiently high emission site density (ESD) for the application, good

stability, and long lifetime. However, most materials that meet requirements of robustness and long-term stability in a sealed vacuum environment also have a large (~5 eV) work function (metals such as Mo) or large electron affinity (semiconductors such as Si) so that a high electric field is required to extract electrons. Consequently, cold cathodes usually have been fabricated as arrays of gated microtips ("Spindt tip" arrays [3]) in which each sharp tip has a very small (often ~ nanometers) radius of curvature in relation to its height, in order to produce a large geometrical enhancement factor (GEF) for the local electric field, as well as the required ESD.

An alternative approach that would completely eliminate the complicated and expensive fabrication of large, high-density arrays of FE tips is to use a thin-film cathode material that has either a very low electron affinity or *intrinsic* nanostructure to provide a sufficiently high GEF. For example, diamond is a wide band gap semiconductor that can have a negative electron affinity surface (conduction band edge above the vacuum level), which should permit electron emission at very low electric fields [4,5]. However, reliable n-type doping of diamond has not been achieved. Consequently, populating and transporting electrons through conduction band states (necessary for field emission) has not been possible and single-crystal diamond is not a good field emitter. Recently, however, a number of carbon-based thin-film materials have been reported to exhibit a low E_{th} and other encouraging FE characteristics. These include carbon nanotubes [6], chemical vapor deposition (CVD) diamond films [7], nanodiamond coatings [8], "coral-like" carbon films [9] and our own hot-filament CVD carbon films [10]. The emission mechanism is not fully understood for these materials but is believed to involve substantial local electric field enhancement, either due to nanostructure (large GEF) that is intrinsic or produced by the deposition process, or to highly nonuniform electronic properties [11] over nanometer distances that produce a locally strong emission site embedded in a non-emitting matrix. Better determinations and understanding of the ESD also are needed in order to realize practical applications for most of these materials (see below).

In this paper we report FE results for a variety of carbon-film materials that were selected to explore the relative importance of nanostructure and of doping for FE from carbon. Results are reported and compared for the following materials:

(1) Undoped, hydrogen-free amorphous carbon films were deposited on n-type Si(001) by ArF (193 nm) pulsed-laser ablation (PLA) of a pyrolytic graphite target. Similar hydrogen-free films have been deposited by two other energetic-beam methods, filtered cathodic vacuum arc deposition (FCVA) and mass-separated ion beam deposition (MSIBD). These energetic-beam-deposited films are very smooth and have variable sp^3 content that is controlled by the carbon-ion deposition energy. The films range from amorphous diamond (a-D), also known as tetrahedral amorphous carbon (ta-C), with up to 85% sp^3 bonding, to mainly graphitic amorphous carbon (a-C) with ≥75% sp^2-bonding. However, FE measurements from a-D have been controversial. Some authors have suggested that a-D is electronically inhomogeneous, consisting of highly sp^3 clusters or "nodules" (with reduced electron affinity) in an sp^2 matrix [12], or alternatively of "tip-like" conducting sp^2 channels penetrating through an sp^3 film [13]. Field emission from both regions has been claimed by different authors [12–14] despite the fact that highly sp^3–bonded a-D is a good insulator. A correlation also has been observed between increasing film roughness (at low deposition energy) and a lower E_{th} for FE [15]. In addition, several groups have demonstrated that ultrathin a-D coatings (ranging from ~2 nm to ~30 nm) can enhance FE from Spindt tip arrays [16–19]. This may be a hot-electron effect with the electrons injected from a metallic substrate layer and tunneling through the a-D coating [18].

(2) Cs-doped amorphous carbon films (a-C:Cs) were produced by direct metal ion beam deposition (DMIBD), in which a primary Cs^+ beam generates the secondary, energetic C^-

deposition beam in the presence of residual Cs vapor [20,21]. These films also have variable sp^2/sp^3 content depending on the incident C^- ion energy [22,23], and for energies in the 50–150 ev range also are extremely smooth [22]. DMIBD films also have been reported to have a FE threshold field as low as 7 V/μm and stable FE characteristics despite the reported high concentration (10%–25%) of normally reactive Cs [24]. An important issue is to better understand the structure of these films and whether Cs actually is incorporated as a dopant.

(3) Deliberately nanostructured carbon films were produced by hot-filament CVD. We recently reported low FE threshold fields ($E_{th} \geq 9$ V/μm) and a high ESD (> 10^5 cm^{-2}) for these films [10]. These characteristics are attributed to intrinsic nanostructure created during the deposition process, as opposed to localized emitting defects produced by "conditioning" during FE testing [10] (see results and discussion below).

(4) Vertically aligned carbon nanotube (CNT) films were grown by dc glow-discharge plasma-enhanced CVD, with the CNT growth catalytically controlled by electron-beam evaporated and plasma-etched transition metal nuclei (Ni or Fe). Details of the CNT growth process are reported elsewhere [25]. Despite having a high work function (similar to graphite, ~4.6 eV), oriented CNTs may be the "ultimate" nanostructured field emitters if their diameter/height ratio, growth-related defects and electrical properties can be controlled precisely to produce a high GEF. Some preliminary FE measurements have been carried out on oriented CNTs and are presented below for comparison with the other materials.

EXPERIMENTAL

Energetic-Beam Deposition of Carbon Films

Carbon films with their sp^3-bonding fraction controlled by the incident-ion kinetic energy were deposited on n-type (001) Si substrates both by ArF (193 nm) pulsed-laser ablation (PLA) of a pyrolytic graphite target, and by direct metal ion beam deposition (DMIBD). The PLA films were undoped while the DMIBD films contained Cs (see below).

Pulsed Laser Deposition (PLD) and Film Characterization

The two PLA systems and the procedures used in this work have been described elsewhere [26–28]. Briefly, films were deposited in vacuum chambers evacuated by turbomolecular pumps to a base pressure of 3 x 10^{-8} Torr. The pulsed ArF (193 nm) laser beam was incident at 45° onto 2.54-cm diameter pyrolytic graphite targets containing < 10 ppm total impurities (Specialty Minerals, Inc., Easton, PA). A lens was positioned at its focal distance from the target, which rotated continuously (20 rpm) during ablation. An important simplification in this work was that, because the short-wavelength ArF laser was used, the ablated flux consisted primarily of *monatomic* ionized and neutral carbon species [29,30]. Consequently, an ion probe could be used to measure the travel time of the ablated ions and, knowing their mass, to infer their mean kinetic energy [26–28]. The time corresponding to the arrival of the ion current peak ("icp") was used to calculate a velocity and corresponding kinetic energy, KE_{icp}, for the ions arriving at the position of the substrate [27]. This information was used to make the first systematic studies of changes in the bonding, optical properties, and surface morphology of pulsed-laser deposited a-D films as a function of the KE_{icp} of the incident species [26–28].

Electron energy loss spectroscopy (EELS) measurements revealed that both the sp^3-bonded carbon fraction and the plasmon peak energy (which is proportional to electron

density or film density) were maximized in films deposited at $KE_{icp} \sim 90$ eV, as shown in Fig. 1. The maximum sp^3–bonding fraction was limited to ~73%, probably because the PLA plume does not consist of monoenergetic C^+ ions but instead contains a distribution of kinetic energies [27]. Spectroscopic ellipsometry measurements showed that the optical (Tauc) energy gap also was maximized (~2.0 eV) in a-D films deposited with $KE_{icp} \sim 90$ eV [26,27].

Tapping-mode atomic force microscope (TM-AFM) measurements revealed that all of the PLD films were extremely smooth (rms roughness of 1-2 Å), but those deposited at the optimum $KE_{icp} \sim 90$ eV had rms roughness of <1 Å over distances of several hundred nm [27]. A small but distinct increase of surface roughness with decreasing C^+ ion kinetic energy was correlated with the increased sp^2–bonding (graphitic) fraction and the relative absence of diamond-like properties [27].
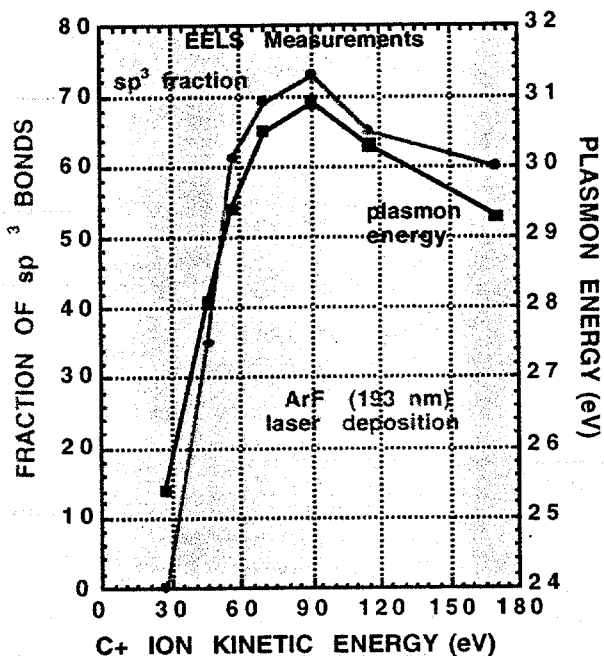

Fig. 1 EELS measurements showing the fraction of sp^3 bonds and the plasmon energy, as functions of the C^+ ion kinetic energy, KE_{icp}, used during ArF-laser deposition [Refs. 26–28].

Direct Metal Ion Beam Deposition (DMIBD) and Film Characterization

Amorphous carbon films with variable sp^3–bonding fraction also were synthesized by extracting a Cs^+ ion beam from a solid source and using it to bombard a graphite target, to produce the negatively charged secondary C^- beam used for film deposition [20,21,31]. A neutral Cs flux (estimated as a few percent of the C^- flux [24]) also was incident on and incorporated in the carbon films. The energy spread of the C^- beam is less than ±5% of the beam energy, while the beam diameter is 2 to 30 mm depending on the beam energy and focusing [20,21]. The negative metal-ion current and deposition energy can be independently controlled in the range of 10–300 eV while maintaining high vacuum (~10^{-9} Torr) [20,21].

The experiments reported here were carried out on a-C:Cs films deposited at C^- energies of 25, 50, 75, 100, 125 and 150 eV. The deposition time was chosen to obtain a film thickness of ~30 nm, since earlier FE measurements on nitrogen-doped amorphous diamond films produced by the filtered cathodic vacuum arc method showed that the 1-nA threshold electric field was minimized for this thickness [32]. (However, the "sphere-to-plane" electrode configuration was used in those measurements, with a 5 mm diam steel anode positioned 40 μm from the film; see the discussion of FE measurements below.)

Spectroscopic ellipsometry (SE) was used to determine the actual thickness and optical constants of the a-C:Cs films. In contrast to the PLA a-D films, it was not possible to obtain good fits when modeling the SE data for a-C:Cs. To model these films it was necessary to

assume that their properties vary with depth, but even at the silicon substrate the film density (~ index of refraction) was less than for the ArF-laser deposited undoped a-D films. This is not surprising since the Cs atom is much larger than C (~3 Å vs ~1 Å), so must tremendously distort an amorphous carbon film. The model finally used to estimate the thickness and density of the a-C:Cs films assumes that the film properties vary over a six-sigma range from the substrate to the film's front surface. Taking three-sigma as the estimated film thickness yielded a thickness of ~19 nm.

An independent estimate of film thickness also was obtained from the depth-integrated measurements of carbon concentration, by dividing by an assumed film density. Assuming the density of graphite (2.26 g/cm^3) yields a film thickness of 11($\pm$1) nm. For this result to be consistent with the ~19 nm thickness determined by SE, the actual film density must be significantly less than that of graphite. We note that the results reported here, as well as the much higher Cs concentrations reported by others earlier [24], become more consistent if the DMIBD a-C:Cs films have a low density that increases from front surface to substrate with the Cs segregated to the near-surface region.

A combination of Rutherford Backscattering Spectrometry (RBS) and nuclear reaction analysis was used to determine the Cs content of the a-C:Cs films. The Cs signal was easily detected by RBS so the results are expected to be accurate to within a few percent. However, because the films were quite thin, the C RBS signal was small and was superimposed on the Si (substrate) signal, which made it difficult to separate the C signal from background noise in all but a few cases. Consequently, nuclear reaction analysis was used instead to determine the C concentration. The results for both Cs and C were expressed as depth-integrated effective surface concentrations (in units of 10^{15} atoms/cm^2), from which the relative Cs concentration was obtained simply as a ratio. Results of the Cs concentration measurements are shown in Fig. 2 for three different sets of samples. For all but one of the samples the Cs concentration was less than 1%. For the five samples for which detailed SE and FE measurements were carried out (see

above and below) the Cs concentration was 0.6($\pm$0.15)%. This value is far below the Cs concentrations ranging from 10% to 25% that were estimated earlier by others from Auger spectroscopy measurements on DMIBD a-C:Cs films [24]. However, as noted above, there may be better consistency between the results reported here and the earlier measurements if the composition and density of the a-D:Cs films varies substantially from front surface to the silicon interface, with the Cs segregated toward the front surface. In that case, surface-sensitive Auger measurements should detect a considerably higher Cs concentration, while our depth-integrated measurements would give an average concentration. Auger electron spectroscopy (AES) measurements revealed that a-C:Cs films deposited on
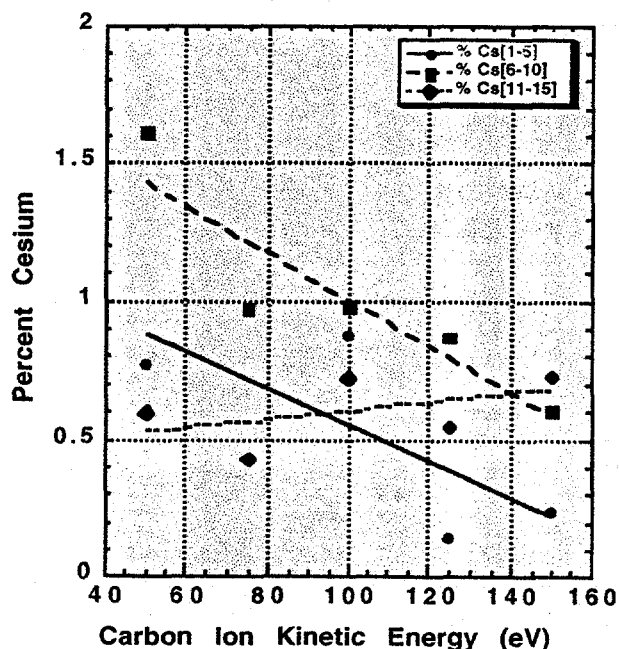

Fig. 2 Cs concentration in DMIBD a-C:Cs films (see text).

Si at room temperature first form a SiC interlayer about 10 atomic layers thick [33]. Further deposition results in a sp^3– or sp^2–rich film depending on the C$^-$ ion energy [33]. However, no information was obtained regarding the Cs distribution in those films.

Hot-Filament CVD Film Deposition and Characterization

HF-CVD carbon films were deposited in a vacuum chamber with a base pressure < 1 x 10^{-7} Torr [34]. A tungsten filament (0.3 mm diam) was located ~5 mm above the n-type (001) Si substrates used for deposition . The filament current was 7 A and the sample temperature during deposition was 570–600°C, as measured by a thermocouple attached directly to the sample surface. This temperature was chosen because it is below the softening point of glass substrates that are considered desirable for deposition of cathode materials for FE displays. An ethylene (C$_2$H$_4$) gas stream was directed onto the filament using a stainless-steel nozzle. The chamber pressure during deposition was 1.2 x 10^{-4} Torr and the deposition rate was ~100 Å/min, as determined by post-deposition profilometry measurements.

Raman scattering measurements were performed on the HF-CVD carbon films to elucidate their structure. They were quite opaque since the Si substrate peak at ~520 cm^{-1} was obscured, indicating the metallic, sp^2-bonded nature of these films. They also were opaque in the infrared. Their Raman spectrum consisted of two broad peaks at ~1350 cm^{-1} and 1600 cm^{-1}. This is characteristic of graphitic, nanocrystalline carbon with a grain size <25 Å, which is the expected form of carbon at our relatively high substrate temperature ~600°C. High-resolution SEM measurements also were carried out as described below.

Field Emission (FE) Measurements

FE measurements were carried out in a vacuum chamber with a base pressure of 10^{-6} Torr by applying a positive voltage to a scanned WC current probe (anode) and collecting the electrons emitted by the sample (cathode). The current probe was mounted on an *x-y-z* translation stage with a minimum step size of 75 nm, which provided precise control of the probe-substrate separation as well as the probe position in the sample plane. In the course of these experiments current-probe tip diameters of ~25 μm, ~5 μm and ~1 μm were used and some of the FE results obtained using different tip diameters were compared (see below). Using these tips it is possible to make contour plots of E$_{th}$ vs location on the film surface and to observe ESDs up to ~10^8 cm^{-2}.

We note that FE measurements often are made using a parallel-plate anode geometry, in which an anode plate with ≥ cm^2 dimensions is separated from the film by calibrated spacers (glass fibers or disks). This method has the great drawback for materials studies that it always collects current from the sample's "hottest" (lowest threshold field) emitting spot, which is frequently a defect. Consequently, the parallel-plate method provides no reliable information about the average FE properties of the emitting material. Similarly, no information is obtained about the emission site density (ESD) unless a phosphor-coated anode is used to directly image the emitting sites, but even then the spatial resolution may be limited by the phosphor and/or recording conditions. A similar concern arises even with the scanned-probe method if the probe has a large tip diameter, e.g. if a rod terminating in a ≥ mm-scale spherical ball is held only tens of μm from the sample. In that case, it has been shown that the measured threshold (turn-on) voltage for FE depends strongly on the tip diameter [35]. The parallel-plate method also has the disadvantage that it is difficult to distinguish leakage current across the spacers that separate anode and cathode from the true FE current. Consequently, it is nearly meaningless to advertise a low threshold voltage for a particular material, if measured only by the parallel-plate method. It
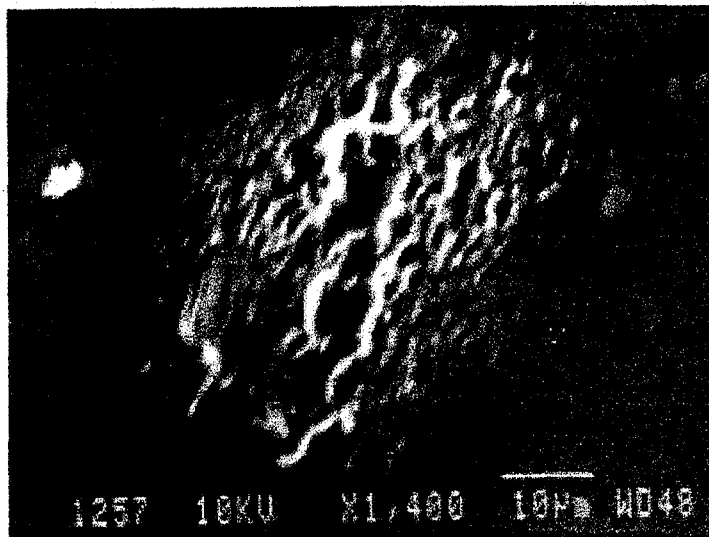
Fig. 3 Crater containing once-molten C and Si at the location where arcing occurred during FE testing of an ArF-laser deposited a-D film.

is for these reasons that we believe only a point probe with three translational degrees of freedom and a diameter smaller than the ESD, or a phosphor screen with known spatial resolution to directly demonstrate the existence of numerous simultaneously emitting sites, should be used as the anode for FE measurements.

FIELD EMISSION RESULTS AND DISCUSSION

FE from Pulsed-Laser Deposited Films

The very smooth, undoped PLD amorphous carbon films were poor field emitters regardless of their sp^3 content [34,36]. "Conditioning" always was required to obtain emission from a-D samples with high sp^3 content and always resulted in striking an arc between the probe tip and the film, as the electric field was increased to 100–200 V/μm. Subsequent SEM measurements revealed that a crater consisting of once-molten C and Si was formed at the location of the arc, as shown in Fig. 3. After arcing, an electric field of ~50 V/μm was required to draw a FE current of 1 nA. This field strength is substantially larger than is needed for FE from the nanostructured carbon materials listed above [6–10] and discussed further below. Nearly as smooth and predominantly sp^2-bonded amorphous C films were deposited using low-kinetic energy (~25 eV) C ions and exhibited very similar FE characteristics but with lower fluctuations of the emitted current.

The emitted currents followed approximately the Fowler-Nordheim (FN) behavior [37] as shown in Fig. 4. From a simplified FN equation [3], and assuming that these amorphous carbon films have a work function equal to that of graphite (4.6 eV), the geometrical enhancement factor (GEF) and effective area of the emitting sites were estimated. For both the highly sp^3-bonded and mainly sp^2-bonded films a high GEF ~100–150 and a low emitting area $>10^{-2}$ μm^2 were inferred. From the combination of (1) the absence of significant FE without conditioning, (2) the very similar behavior of amorphous carbon films after arcing, regardless of their sp^3 content, and (3) the change from extremely smooth films (as seen by AFM) before arcing to films with craters and a high GEF after arcing, we conclude that the FE from amorphous carbon films is due to the sharp protrusions around the craters formed during arcing. These protrusions produce a local
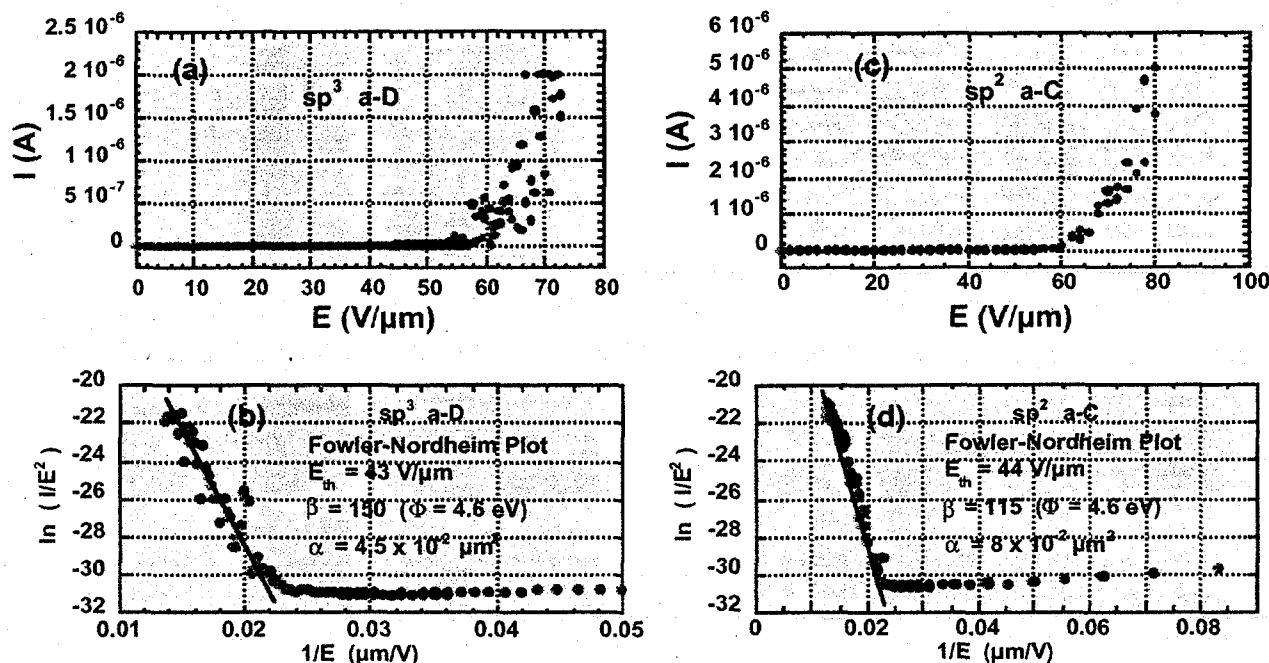
Fig. 4 (a) FE current vs applied field and (b) FN plot for a high-sp^3 a-D film deposited at KE_{icp} ~90 eV. (c) and (d) show similar results for a mainly sp^2-bonded a-C film deposited at KE_{icp} ~25 eV.

geometrical enhancement of the applied electric field, resulting in FE at moderate applied fields, but this FE is not intrinsic or characteristic of uniform films.

FE from Cs-Containing DMIBD Films

FE measurements were carried out for a-C:Cs films deposited on both smooth and textured Si substrates. The films deposited at C$^-$ kinetic energies of 50, 75, 125 and 150 eV on smooth Si substrates were essentially non-field emitters. Electron emission always was accompanied by an arc between the probe tip and the film at electric fields of 120–200 V/µm. I-E data could be obtained only after arcing; consequently this FE is considered to originate from the protrusions surrounding the crater formed by arcing and thus is not representative of emission from a smooth a-D:Cs film. After arcing, the emission thresholds for 1 nA current were in the range of 60–115 V/µm.

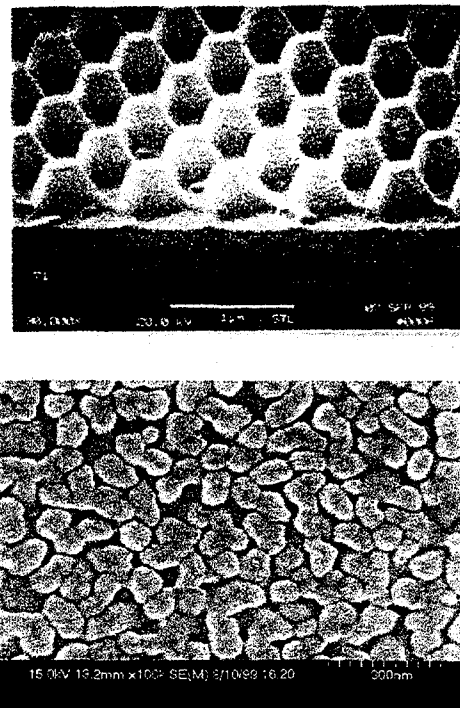In contrast, a-D:Cs films deposited on several different types of textured Si surfaces

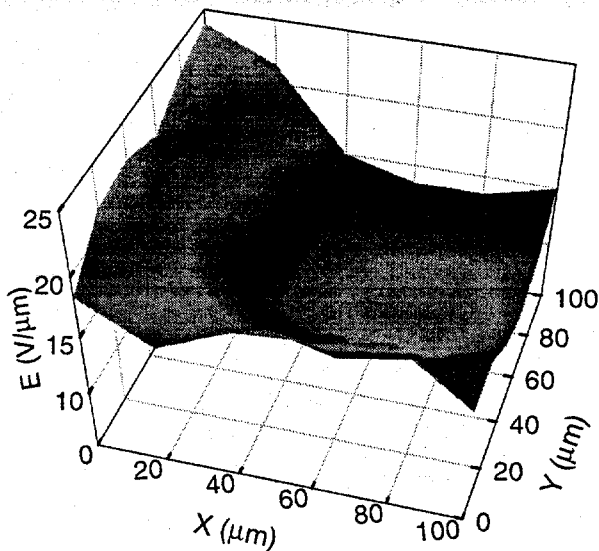**Fig. 5** Textured Si surfaces produced by (top) laser holography and (bottom) the HSG process.

Fig. 6 Contour plot over a 100 μm x 100 μm area showing the electric field, E_{th}, required to extract 1 nA current from a HF-CVD film, using the 25-μm diam probe at a distance of 20 μm from the sample.

generally produced FE without the need for conditioning and the accompanying arcing. The textured Si surfaces were produced by laser holography (laser interference patterning of photoresist followed by reactive ion etching with SF_6), by wet etching, and by the HSG process [38]. Figure 5 shows two of the surfaces on which a-D:Cs films were deposited for FE measurements. However, field strengths > 50 V/μm were required to emit 1 nA current from the a-D:Cs coatings on all of these textured surfaces, so they are still not competitive with the HF-CVD or carbon nanotube films described below.

There is a striking discrepancy between the FE results for our a-D:Cs films and the very low FE threshold field ≥ 7 V/μm and stable FE characteristics reported by Bozorth et al [24], as well as their much higher reported Cs concentration (10%–25% vs our < 1%). They also reported that FE from a-D:Cs was stable for periods up to 6 months, despite the reported high concentration of normally highly reactive Cs [24]. One possibility, of course, is that the differences are genuine and result from different film deposition procedures. For example, their films may have been much thicker than our relatively thin (~19 nm) films with varying density; perhaps thicker films are able to incorporate more Cs. However, no thickness is mentioned for their films. Moreover, their estimated Cs flux was only ~3% of the C flux during film deposition, which seems at least superficially inconsistent with the very high Cs content that they estimated from surface-sensitive Auger spectroscopy.

FE from HF-CVD Carbon Films

In contrast to the energetic-beam deposited a-D and a-C films just described, the HF-CVD C films exhibited very promising FE characteristics. (1) No conditioning or arcing was required to initiate emission, once the threshold voltage
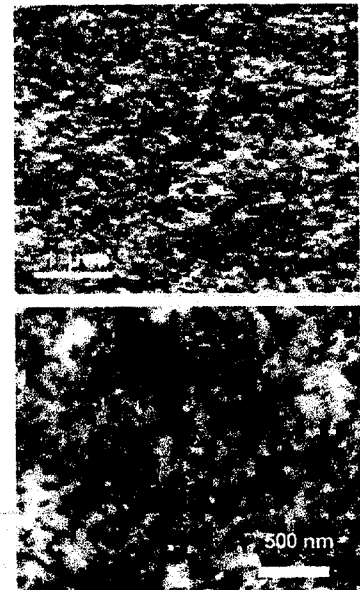

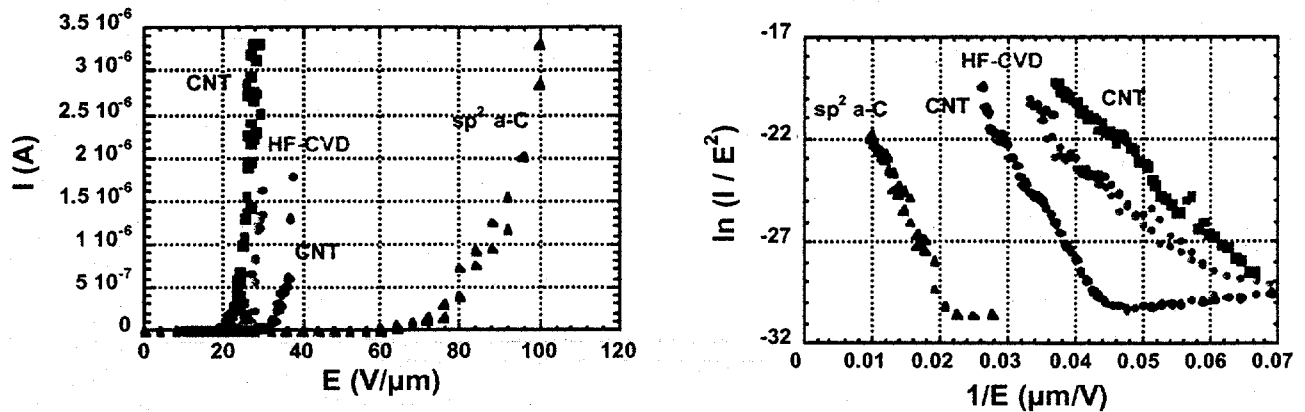**Fig. 7** Field emission SEM images of an HF-CVD C

Fig. 8 (Left) Current vs applied field and (right) FN plot for several carbon-film materials deposited on Si substrates.

was reached. (2) No significant hysterisis was observed, suggesting a nondestructive FE mechanism. (3) Turn-on voltages (for 1 nA current) were quite low, ranging from 9 to 30 V/μm. (4) As illustrated in Fig. 6, by laterally scanning the 25 μm-diam probe tip the HF-CVD films were found to be *continuously* emitting, though with some variation of threshold voltage. The intrinsic ESD of HF-CVD films implied by these measurements is quite high, at least 3×10^5 cm^{-2}. (5) The maximum FE current before damage was 5–50 μA, corresponding to a macroscopic current density ~1–10 A-cm^{-2}. (6) The emitted current was stable for 30–50 hours, the maximum time for which measurements were made.

The high-resolution SEM images shown in Fig. 7 reveal that HF-CVD films having good FE characteristics are highly nanostructured, with many features in the 100 nm range and smaller. An important question is whether these attractive FE characteristics result primarily from the HF-CVD films higher (~570–600°C) deposition temperature, in comparison with the a-D and a-C films deposited at room temperature. To test this possibility PLD was used to deposit a-C films from energetic C$^+$ ions at T ~600–700°C. The resulting films were nanocrystalline (like HF-CVD films) but were very smooth and still exhibited poor FE characteristics.

Figure 8 compares the FE characteristics of an HF-CVD film and a laser-deposited (mainly sp^2-bonded) a-C film with preliminary FE measurements for two vertically aligned carbon nanotube films grown by a plasma-assisted CVD process [25]. The measurements were carried out using the 25-μm diam probe, but no differences were observed when the 5-μm diam probe was used to repeat the measurements for the CNT films. It can be seen that the HF-CVD film is highly competitive with the nanotube films and that both are considerably better than the laser-deposited a-C.

We conclude that the excellent FE from HF-CVD C films is associated with their nanostructure and the associated large GEF, despite their high work function of ~4.6 eV. The absence of conditioning, their low turn-on voltage and high ESD, and the apparent durability of the HF-CVD films are promising for FE displays and other vacuum microelectronic devices.

SUMMARY

The hydrogen-free and very smooth a-D or a-C films (with high or low sp^3 content) produced by PLD, (as well as other energetic-beam methods), are not good field emitters. Conditioning is required to obtain emission, accompanied by arcing, so that their subsequent FE is characteristic of the arc-produced damage site. PLD films deposited in the same 600–700°C temperature range as HF-CVD carbon films were still very smooth (though nanocrystalline) and still exhibited poor FE characteristics. The incorporation of ~1% Cs in thin (~20 nm) DMIBD a-C films also was found not to improve their FE characteristics. However, even modest surface texturing can eliminate the need for conditioning, presumably by geometrical enhancement of the local electric field, though the FE threshold for a-D:Cs coatings on textured Si remained > 50 V/μm, which is not competitive with nanostructured forms of carbon.

The most promising approach for producing macroscopically flat FE cathodes is to use materials that are highly nanostructured, either intrinsically (e.g. carbon nanotubes) or by the deposition process (e.g. HF-CVD carbon). HF-CVD films were shown to combine a number of desirable properties for FE displays and vacuum microelectronics, including the absence of conditioning, low turn-on fields, high emission site density, and apparent stability and durability during limited testing. We conclude that the excellent FE from HF-CVD C films is associated with their nanostructure and the associated high GEF, despite their high (graphitic) work function. Preliminary FE measurements also revealed that vertically aligned carbon nanotubes are equally promising. Research is continuing in order to optimize the FE characteristics of these two highly nanostructured forms of carbon.

ACKNOWLEDGMENTS

REFERENCES

1. See for example J. H. Jung, B. K. Ju, Y. H. Lee, J. Jang, and M. H. Oh, *IEEE Elec. Dev. Lett.* **18**, 197 (1999).
2. See for example A. A. G. Driskill-Smith, D. G. Hasko, and H. Ahmed, *Appl. Phys. Lett.* **75**, (1999).
3. C. A. Spindt, I. Brodie, L. Humphrey, and E. R. Westerberg, *J. Appl. Phys.* **47**, 5248 (1976).
4. F. J. Himpsel, J. A. Knapp, J. A. Van Vechten, and D. E. Eastman, *Phys. Rev. B* **20**, 624 (1979).
5. J. Van der Weide, and R. J. Nemanich, *Appl. Phys. Lett.* **62**, 1878 (1993).
6. W. A. de Heer, A. Chatelain, and D. Ugarte, *Science* **270**, 1179 (1995).
7. D. Zhou, A. R. Krauss, T. D. Corrigan, T. G. McCauley, R. P. H. Chang, and D. M. Gruen, *J. Electrochem. Soc.* **144**, 224 (1997).
8. W. Zhu, G. P. Kochanski, and S. Jin, *Science* **282**, 1471 (1998).

9. B. F. Coll, J. E. Jaskie, J. L. Markham, E. P. Menu, A. A. Talin, and P. von Allmen, p. 185 in *Covalently-Bonded Disordered Thin-Film Materials*, ed. by M. P. Siegal, W. I. Milne, and J. E. Jaskie, Materials Research Society, Warrendale, PA, 1998.

10. V. I. Merkulov, D. H. Lowndes, and L. R. Baylor, *Appl. Phys. Lett.* **75**, 1228 (1999).

11. J. Robertson, *J. Vac. Sci. Technol. B* **17**, 659 (1999).

12. F. Y. Chuang, C. Y. Sun, T. T. Chen, and I. N. Lin, *Appl. Phys. Lett.* **69**, 3504 (1996).

13. O. Groning, O. M. Kuttel, P. Groning, and L. Schlapbach, *Appl. Surf. Sci.* **111**, 135 (1997).

14. A. V. Karabutov, V. I. Konov, V. G. Ralchenko, E. D. Obraztsova, V. D. Frolov, S. A. Uglov, H.-J. Scheibe, V. E. Strelnitskij, and V. I. Polyakov, *Diamond and Related Mater.* **7**, 802 (1998).

15. C. Park, H. Park, Y.-K. Hong J. S. Kim, and J. K. Kim, *Appl. Surf. Sci.* **111**, 140 (1997).

16. J. H. Jung, B. K. Ju, Y. H. Lee, J. Jang, and M. H. Oh, *IEEE Elec. Dev. Lett.* **18**, 197 (1997).

17. V. G. Litovchenko, A. A. Evtukh, R. I. Marchenko, N. I. Klyui, and V. A. Semenovich, *Appl. Surf. Sci.* **111**, 213 (1997).

18. N. S. Xu, J. C. She, S. E. Huq, J. Chen, and S. Z. Deng, *Appl. Phys. Lett.* **73**, 3668 (1998).

19. J. C. She, S. E. Huq, J. Chen, S. Z. Deng, and N. S. Xu, *J. Vac. Sci. Technol. B* **17**, 592 (1999).

20. Y. Park, Y. W. Ko, M. H. Sohn, and S. I. Kim, *Mater. Res. Soc. Symp. Proc.* **396**, 623 (1996).

21. S. I. Kim, *Rev. Sci. Instr.* **67**, 908 (1996).

22. M. H. Sohn, Y. O. Ahn, Y. W. Ko, S. R. Hah, T. E. Fischer, and S. I. Kim, *J. Vac. Sci. Technol. A* **16**, 3554 (1998).

23. Y. W. Ko and S. I. Kim, *J. Vac, Sci, Technol. A* **15**, 2750 (1997).

24. S. P. Bozeman, S. M. Camphausen, J. J. Cuomo, S. I. Kim, Y. O. Ahn, and Y. Ko, *J. Vac. Sci. Technol. A* **15**, 1729 (1997).

25. V. I. Merkulov, D. H. Lowndes, Y. Y. Wei, and G. Eres, "Patterned growth of individual and multiple vertically-aligned carbon nanotubes," submitted to *Applied Physics Letters*.

26. D. H. Lowndes, V. I. Merkulov, A. A. Puretzky, D. B. Geohegan, G. E. Jellison, Jr., X. M. Rouleau, and T. Thundat, *Mat. Res. Soc. Symp. Proc.* **526**, 325 (1998).

27. D. H. Lowndes, V. I. Merkulov, A. J. Pedraza, J. D. Fowlkes, A. A. Puretzky, D. B. Geohegan, and G. E. Jellison, Jr., Symposium on Surface Engineering: Science and Technology I, Proc. of TMS 1999 Annual Meeting, 1999 (in press).

28. V. I. Merkulov, D. H. Lowndes, G. E. Jellison, Jr., A. A. Puretzky, and D. B. Geohegan, *Appl. Phys. Lett.* **73**, 2591 (1998).

29. A. A. Puretzky et al., *Appl. Surf. Sci.* **96-98**, 859 (1996).

30. D. B. Geohegan and A. A. Puretzky, *Mat. Res. Soc. Symp. Proc.* **397**, 55 (1996).

31. This method of producing a C⁻ beam was developed by SKION Corp. and has been used to produce negative-ion beams of several metals.

32. R. D. Forrest, A. P. Burden, S. R. P. Silva, L. K. Cheah, and X. Shi, *Appl. Phys. Lett.* **73**, 3784 (1998).

33. Y. W. Ko and S. I. Kim, *J. Vac. Sci. Technol. A* **15**, 2750 (1997).

34. V. I. Merkulov, D. H. Lowndes, and L. R. Baylor, *Appl. Phys. Lett.* **75**, 1228 (1999).

35. A. Gohl, A. N. Alimova, T. Habermann, A. L. Mescheryakova, D. Nau, V. V. Zhirnov, and G. Muller, *J. Vac. Sci. Technol. B* **17**, 670 (1999).

36. V. I. Merkulov, D. H. Lowndes, and L. R. Baylor, "Field emission and nanostructure of carbon films," submitted to Amorphous and Nanostructured Carbon, Symposium U of the Fall, 1999 MRS meeting, Boston, MA (in press).

37. R. H. Fowler and L. W. Nordheim, *Proc. Roy. Soc. London, Ser. A* **119**, 173 (1928).

38. Further information can be obtained from SKION Corp.